



J Nat Sci Biol Med. 2015 Jul-Dec; 6(2): 335–339.

PMCID: PMC4518404

doi: [10.4103/0976-9668.159998](https://doi.org/10.4103/0976-9668.159998)

Toxic effects of Mn₂O₃ nanoparticles on rat testis and sex hormone

[Masoud Negahdary](#), [Zahra Arefian](#),¹ [Hajar Akbari Dastjerdi](#),¹ and [Marziyeh Ajdary](#)²

Yazd Cardiovascular Research Center, Shahid Sadoughi University of Medical Sciences, Yazd, Iran

¹*Department of Biology, Payame Noor University, Isfahan, Iran*

²*Young Researchers and Elite Club, Khorasgan Branch, Islamic Azad University, Isfahan, Iran*

Address for correspondence: Dr. Marziyeh Ajdary, Young Researchers and Elite Club, Khorasgan Branch, Islamic Azad University, Isfahan, Iran. E-mail: ajdari_ma1365@yahoo.com

Copyright : © Journal of Natural Science, Biology and Medicine

This is an open-access article distributed under the terms of the Creative Commons Attribution-Noncommercial-Share Alike 3.0 Unported, which permits unrestricted use, distribution, and reproduction in any medium, provided the original work is properly cited.

Abstract

Background and Objective:

The safety of Mn₂O₃ nanoparticles (which are extensively used in industries) on male reproductive system is not known. Hence, we investigated the effects of Mn₂O₃ nanoparticles on male reproductive system.

Materials and Methods:

A total of 40 Wistar adult male rats were randomly assigned to four groups of 10 rats each. Three groups received Mn₂O₃ solution in concentrations of 100, 200, and 400 ppm orally for 14 days; the control group received equal volume of saline solution. Blood samples and testicles were collected for analysis.

Results:

Significant reduction in luteinizing hormone (LH), follicle-stimulating hormone (FSH), testosterone, spermatogonial cells, primary spermatocyte, spermatid and Leydig cell was observed in the Mn₂O₃ nanoparticles treated groups compared with controls.

Conclusion:

Mn₂O₃ nanoparticles significantly reduce FSH, LH, and testosterone levels resulting in a significant reduction in testicular cytology.

Keywords: Follicle-stimulating hormone, luteinizing hormone, Mn₂O₃ nanoparticles, testosterone, toxicity

INTRODUCTION

The advancement in nanotechnology and wide application of nanomaterials have collaterally increased the human exposure to these particles raising concerns on their potential health hazards.[1,2,3] Although a few studies have evaluated the systemic toxicity and distribution of the nanoparticles[4] the diversified nature of nanoparticles requires a through and system specific evaluation. Moreover, the nature of toxicity of nanoparticles, is significantly dose-dependent.[5] Various forms of Mn₂O₃ nanoparticles (tube, wire, plate, sphere and nanoshell shapes) are developed,[6,7] with varying toxic effects. The characteristics of these nanoparticles are influenced by their size.[8,9,10] Mn₂O₃ including MnO, MnO₂, Mn₃O₄ are used as a composite in wastewater treatment, catalyzing, sensors, super capacitors, alkaline, and battery recharging. [11,12,13,14,15] However, in addition to the advantages of nanoparticles in today's industrial applications, the exposure and toxicity of these nanoparticles to human and animal health are collateral,[16] which

necessitates understanding the system specific toxic effects of these nanoparticles. Hence the present study was designed to investigate the effects of Mn₂O₃ nanoparticles on the levels of testosterone (T), follicle-stimulating hormone (FSH), luteinizing hormone (LH), and the testicle cytology of male mice. Bar-shaped nanoparticles with an approximate diameter of 70 nm were used in our study. LH in males stimulates a specific type of Leydig cells in testicles for the production of testosterone. The LH level in the males is consistent after puberty. The increase in testosterone levels gives a negative feedback to the pituitary gland and hypothalamus glands, which results in a decrease of LH secretion. LH secretions and FSH levels for testosterone are the primary tests used for the work-up on infertility in males and females patients.[17]

MATERIALS AND METHODS

Materials

Mn (III) acetylacetonate, Acetone, ethanol, and chloroform were used to prepare nanoparticles. Saline, ketamine, Rat chow, hematoxylin eosin, and laboratory kit (DB52181, Merck. Co., of Germany) were used.

Equipments

X-ray diffraction (XRD), transmission electron microscopy (TEM) (JEM-200CX), ultraviolet (UV)-visible, optical microscope (OLYMPUS CX 21 FS1), and ELISA Reader (HumaReader HS by HUMAN Co., Germany) was used.

Preparation of Mn₂O₃

Mn₂O₃ nanoparticles were first synthesized by providing heat to Mn (III) acetylacetonate (1 mmol, 0.35 g) in 20 mL acetone or ethanol in a Teflon-lined Parr acid-digestion bomb at 200°C for 72 h. The resulting dark solution was distributed into chloroform and centrifuged for 10 min. The residual black solution obtained was isolated and dried under vacuum condition at room temperature for 12 h, following which the calcination process was conducted at 500°C for 4 h. The final product was analyzed by XRD, UV-visible, and TEM (JEM-200CX).

Methods

Totally 40 male Wistar rats weighing 230 ± 20 g were housed at appropriate temperature/light conditions, and were fed standard prepared food consisting of 20% protein, 50% carbohydrate, 10% cellulose, 15% fat and vitamins. The study was approved by the Institute Ethics Committee. Rats were procured from the Isfahan University of Medical Sciences. The rodents were randomly assigned to four groups consisting of 10 rats each. The test-groups 1, 2, 3 received Mn₂O₃ nanoparticle solution in 100, 200, and 400 ppm concentrations respectively for 14 days by orally (gavage), and group 4 as the control-group, which received an oral saline placebo. Applied Mn₂O₃ Nps in this research were of 70 nm diameter. At the end of the trial, the mice were first anesthetized by ketamine and autopsied. For hormone evaluation, the arterial blood samples were collected from the heart and analyzed by commercial ELISA kits (pars azmon). The testicles together with epididymis were dissected and removed and transferred into a physiological saline for further investigation on cellular modifications using an optical microscope. Five different sites from any section were selected and in any field a cross-section of seminiferous tubules was studied. Investigative measurements and cell numerations (spermatogonial cells, primary spermatocyte, spermatid, and Leydig cell) were performed. The raw data were analyzed by SPSS.19 statistical analysis software using ANOVA and Dunnett tests. Statistically, variation of results among observed groups was considered significant at $P < 0.05$.

Tissue processing

Five different sites from each section with a thickness of 2 mm were selected and in any field, and a cross-section of seminiferous tubules was studied. The tissue was fixed in 10% Formalin and processed in various grades of ethanol, xylene, chloroform, toluene eventually for paraffin embedding. The paraffin

embedded tissue was sectioned using a microtome, and the tissue section was mounted on a glass slide for staining using hematoxylin and eosin.[18]

RESULTS

X-ray diffraction of Mn₂O₃ nanoparticles

The XRD pattern for Mn₂O₃ is illustrated [Figure 1](#), and diffraction peaks absorbance is at 2θ values. Dominant peaks are used to estimate grain size of sample contributed by Scherrer equation,[19] $D = K\lambda / (\beta \cos \theta)$ where K is constant (0.9), λ is the wavelength ($\lambda = 1.5418 \text{ \AA}$) (Cu $K\alpha$), β is the full width at the half-maximum of the line and θ is the diffraction angle. Estimated grain size were found to be $\pm 70 \text{ nm}$ using relative intensity peak for Mn₂O₃ nanoparticles and increase in sharpness of XRD peaks implies that particles are crystal shape in nature. All peaks in [Figure 1](#) are associated with Mn₂O₃ nanoparticles and consistent with Joint Committee for Powder Diffraction Studies.[19]

Size distribution and microscopic characterization of Mn₂O₃ nanoparticles

A particle size analyzer was applied to determine the area of sizes of the Mn₂O₃ nanoparticles. [Figure 2](#) demonstrates the size dispersion of one of the arranged Mn₂O₃ nanoparticles. The mean size of the Mn₂O₃ nanoparticles was around $70 \pm 5 \text{ nm}$.

The properties of a wide variety of materials and function of many devices highly depend on their surface characteristics.[20] The morphology of Mn₂O₃ nanoparticles was studied by applying TEM). [Figure 3](#) show the images of sample by TEM.

Mn₂O₃ nanoparticles caused a in the testosterone ($P = 0.001$), LH ($P = 0.004$) and FSH ($P = 0.01$) levels in-group receiving 400 ppm of Mn₂O₃ [[Figure 4a–c](#)].

Significant reduction in the number of spermatogonial cells ($P = 0.007$), primary spermatocyte cells ($P = 0.000$) and spermatid cells ($P = 0.002$) was observed receiving 400 ppm Mn₂O₃ nanoparticles [[Figures 5a–c](#) and [6](#)].

The number of Leydig cells in all groups decreased but were significant in the group receiving 400 ppm dosage ($P = 0.003$) [[Figures 6](#) and [7](#)].

In this investigation, the pathological studies demonstrated 400 ppm dosage leads to

1. An increase in cellular disruption in the seminiferous tubules,
2. Interstitial edema of seminiferous tubules,
3. Appearance of vacuoles in epithelium and
4. A reduction in cell regulation, as shown in [Figure 6a](#).

Irregularities were discovered in germinal cells levels, seminiferous tubules, and thickness reduction of epithelium was observed [[Figure 8c](#)]. In the group receiving 200 ppm Mn₂O₃ nanoparticles, the elevation in cellular disruption of seminiferous tubules was partially obvious. These comparisons were made with the control group [[Figure 8d](#)].

DISCUSSION

The effect of oral intake of Mn₂O₃ nanoparticles in 100, 200, and 400 ppm concentrations on testosterone, LH, FSH, spermatogonial cells, primary spermatocyte, spermatid, Leydig and pathological modifications in the testicle tissue were evaluated. Mn₂O₃ nanoparticles caused malignancies in the testicular tissue, a decrease in the levels of the sex hormones, and spermatogonial cells, primary spermatocyte, spermatid, and Leydig cells at the dose of 400 ppm. Mn₂O₃ in nanoscale may produce active oxygen that results in toxicity via oxidative stress, producing a variety of active oxygen is the dominant mechanism of toxicity raised from Mn₂O₃ nanoparticles. Several studies have demonstrated that cells exposed to Mn₂O₃ nanoparticles, have a lower mitochondrial activity, leading to severe tissue damage.[21,22,23,24] Nanoparticles have severe toxic effects on the male reproduction system by trespassing the blood barrier in

the testicular tissue and damage the sperm cells.[25] Nanoparticles have also been shown to be toxic on stem cells *in vitro* and can interfere with male reproduction system.[26] Nanoparticles may also react with DNA and may lead to inflammation, oxidative stress and impairment in cell function.[27] Titanium nanoparticles were shown to result in infertile sperm, and abnormal Leydig cell[28] while other nanoparticles can accumulate in testicular tissue, including Leydig cell, sertoli cells, and spermatid.[17] The effects of Mn₂O₃ nanoparticles on sex hormone reduction observed in our study could be due to the above factors including direct toxic effects on testicular cytology.

CONCLUSION

We conclude that the Mn₂O₃ nanoparticles at a dose of 400 ppm can reduce sex hormones, sperm production and damage the testicular cytology.

ACKNOWLEDGMENT

We would like to thank Mr. Sadeghi for helping us in this study.

Footnotes

Source of Support: Expenses of this work were discharged by authors.

Conflict of Interest: None declared.

REFERENCES

1. Mirkovic B, Turnsek TL, Kos J. Nanotechnology in the treatment of cancer. *Zdravniski Vestnik*. 2010;79(2)
2. Gupta AK, Gupta M. Synthesis and surface engineering of iron oxide nanoparticles for biomedical applications. *Biomaterials*. 2005;26:3995–4021. [PubMed: 15626447]
3. Pankhurst QA, Connolly J, Jones S, Dobson J. Applications of magnetic nanoparticles in biomedicine. *J Phys D Appl Phys*. 2003;36:167–81.
4. Almeida JP, Chen AL, Foster A, Drezek R. *In vivo* biodistribution of nanoparticles. *Nanomedicine (Lond)* 2011;6:815–35. [PubMed: 21793674]
5. Kong B, Seog JH, Graham LM, Lee SB. Experimental considerations on the cytotoxicity of nanoparticles. *Nanomedicine (Lond)* 2011;6:929–41. [PMCID: PMC3196306] [PubMed: 21793681]
6. Ghosh M, Biswas K, Sundaresan A, Rao C. MnO and NiO nanoparticles: Synthesis and magnetic properties. *J Mater Chem*. 2006;16:106–11.
7. Liu R, Duay J, Lee SB. Redox exchange induced MnO₂ nanoparticle enrichment in poly (3, 4-ethylenedioxythiophene) nanowires for electrochemical energy storage. *ACS Nano*. 2010;4:4299–307. [PubMed: 20590128]
8. Shumakova AA, Trushina ÉN, Mustaphina OK, Soto SKh, Gmshinskii IV, Khotimchenko SA. Influence of titanium dioxide and silica nanoparticles on accumulation and toxicity of lead in experiments with intragastric co-administration. *Vopr Pitan*. 2014;83:57–63. [PubMed: 25059070]
9. Lee GH, Huh SH, Jeong JW, Choi BJ, Kim SH, Ri HC. Anomalous magnetic properties of MnO nanoclusters. *J Am Chem Soc*. 2002;124:12094–5. [PubMed: 12371839]
10. Yin M, O'Brien S. Synthesis of monodisperse nanocrystals of manganese oxides. *J Am Chem Soc*. 2003;125:10180–1. [PubMed: 12926934]
11. Seo WS, Jo HH, Lee K, Kim B, Oh SJ, Park JT. Size-dependent magnetic properties of colloidal Mn(3)O(4) and MnO nanoparticles. *Angew Chem Int Ed Engl*. 2004;43:1115–7. [PubMed: 14983449]
12. Park J, Kang E, Bae CJ, Park JG, Noh HJ, Kim JY, et al. Synthesis, characterization, and magnetic properties of uniform-sized MnO nanospheres and nanorods. *J Phys Chem B*. 2004;108:13594–8.

13. Park J, An K, Hwang Y, Park JG, Noh HJ, Kim JY, et al. Ultra-large-scale syntheses of monodisperse nanocrystals. *Nat Mater*. 2004;3:891–5. [PubMed: 15568032]
14. Richardson J, Yiagas D, Turk B, Forster K, Twigg M. Origin of superparamagnetism in nickel oxide. *J Appl Phys*. 1991;70:6977–82.
15. Bødker F, Hansen MF, Koch CB, Lefmann K, Mørup S. Magnetic properties of hematite nanoparticles. *Phys Rev B*. 2000;61:6826.
16. Dobrzynska MM, Gajowik A, Radzikowska J, Lankoff A, Dušinská M, Kruszewski M. Genotoxicity of silver and titanium dioxide nanoparticles in bone marrow cells of rats *in vivo*. *Toxicology*. 2014;315:86–91. [PubMed: 24321264]
17. Fartkhoni FM, Noori A, Momayez M, Sadeghi L, Shirani K, Babadi VY. The effects of nano titanium dioxide (TiO₂) in spermatogenesis in wistar rat. *Eur J Exp Biol*. 2013;3:145–9.
18. Ayala E, Enghardt MH, Horton M. Cost effective, environmentally safe tissue processing method with paraffin oil. *J Histotechnol*. 1997;20:133–7.
19. Monico L, Van der Snickt G, Janssens K, De Nolf W, Miliani C, Verbeeck J, et al. Degradation process of lead chromate in paintings by Vincent van Gogh studied by means of synchrotron X-ray spectromicroscopy and related methods 1. Artificially aged model samples. *Anal Chem*. 2011;83:1214–23. [PubMed: 21314201]
20. Van Ruitenbeek J, Alvarez A, Pineyro I, Grahmann C, Joyez P, Devoret M, et al. Adjustable nanofabricated atomic size contacts. *Rev Sci Instrum*. 1996;67:108–11.
21. Erikson KM, Dobson AW, Dorman DC, Aschner M. Manganese exposure and induced oxidative stress in the rat brain. *Sci Total Environ*. 2004;334-335:409–16. [PubMed: 15504526]
22. Stokes AH, Lewis DY, Lash LH, Jerome WG, 3rd, Grant KW, Aschner M, et al. Dopamine toxicity in neuroblastoma cells: Role of glutathione depletion by L-BSO and apoptosis. *Brain Res*. 2000;858:1–8. [PubMed: 10700589]
23. Calne DB, Chu NS, Huang CC, Lu CS, Olanow W. Manganism and idiopathic parkinsonism: Similarities and differences. *Neurology*. 1994;44:1583–6. [PubMed: 7936278]
24. Cohen G, Spina MB. Deprenyl suppresses the oxidant stress associated with increased dopamine turnover. *Ann Neurol*. 1989;26:689–90. [PubMed: 2510589]
25. McAuliffe ME, Perry MJ. Are nanoparticles potential male reproductive toxicants? A literature review. *Nanotoxicology*. 2007;1:204–10.
26. Braydich-Stolle L, Hussain S, Schlager JJ, Hofmann MC. *In vitro* cytotoxicity of nanoparticles in mammalian germline stem cells. *Toxicol Sci*. 2005;88:412–9. [PMCID: PMC2911231] [PubMed: 16014736]
27. Nel A, Xia T, Mädler L, Li N. Toxic potential of materials at the nanolevel. *Science*. 2006;311:622–7. [PubMed: 16456071]
28. Ema M, Kobayashi N, Naya M, Hanai S, Nakanishi J. Reproductive and developmental toxicity studies of manufactured nanomaterials. *Reprod Toxicol*. 2010;30:343–52. [PubMed: 20600821]

Figures and Tables

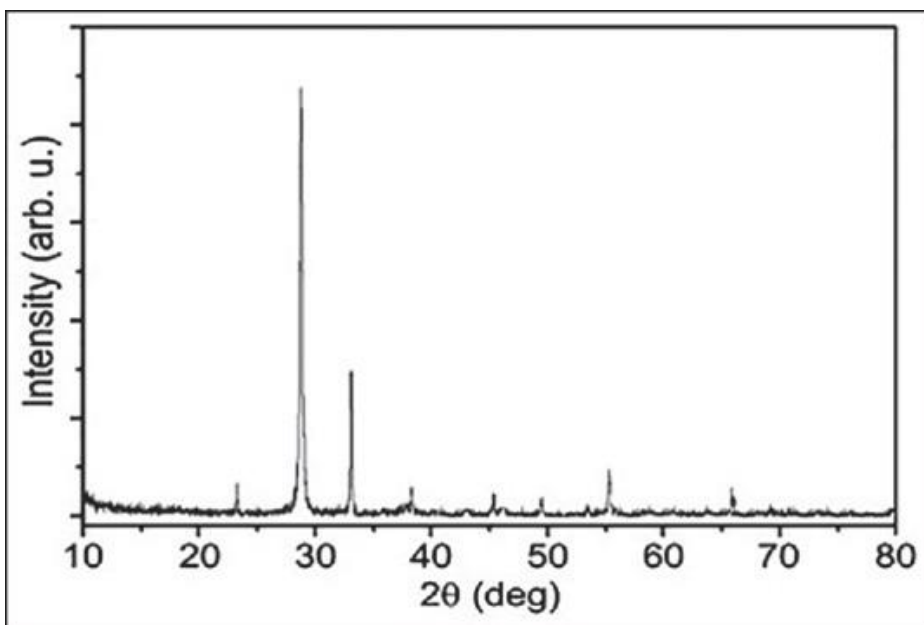
Figure 1X-ray diffraction pattern for Mn₂O₃ nanoparticles

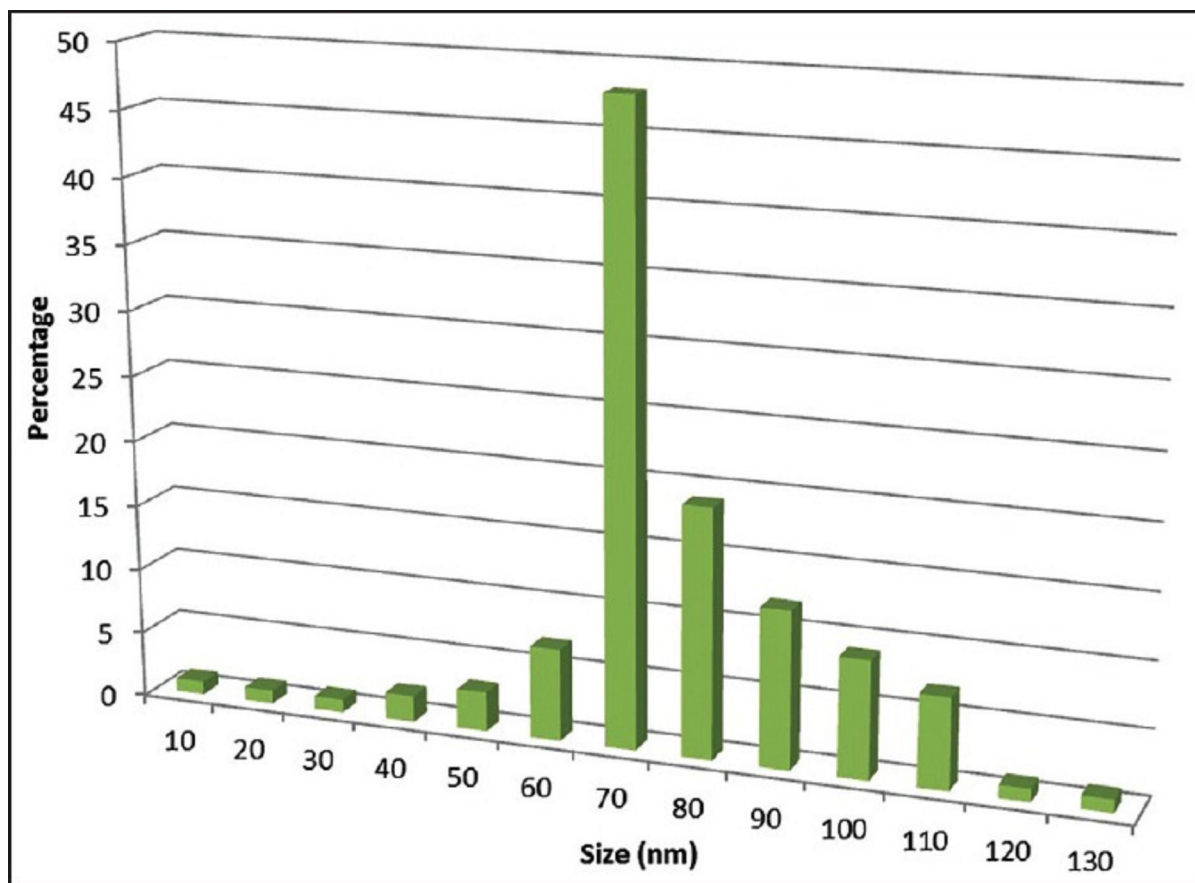
Figure 2Size distribution of Mn₂O₃ nanoparticles

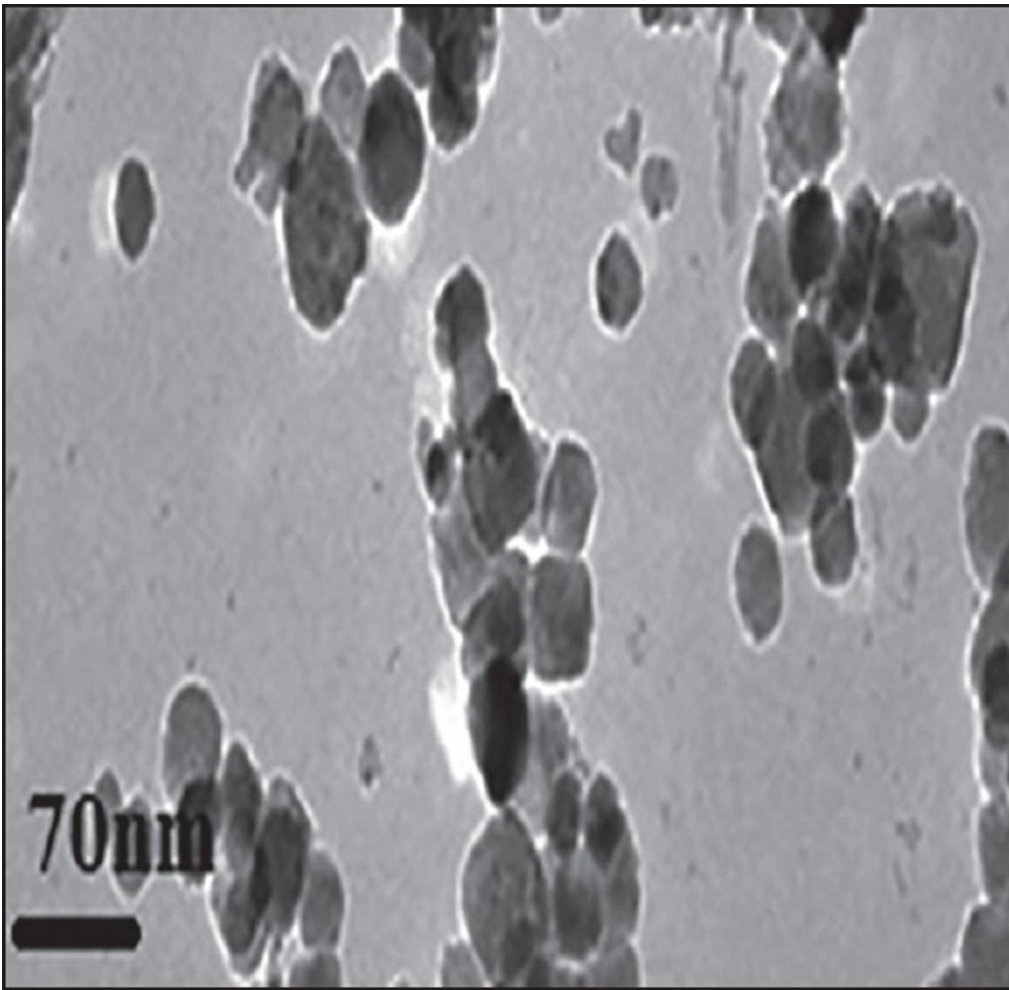
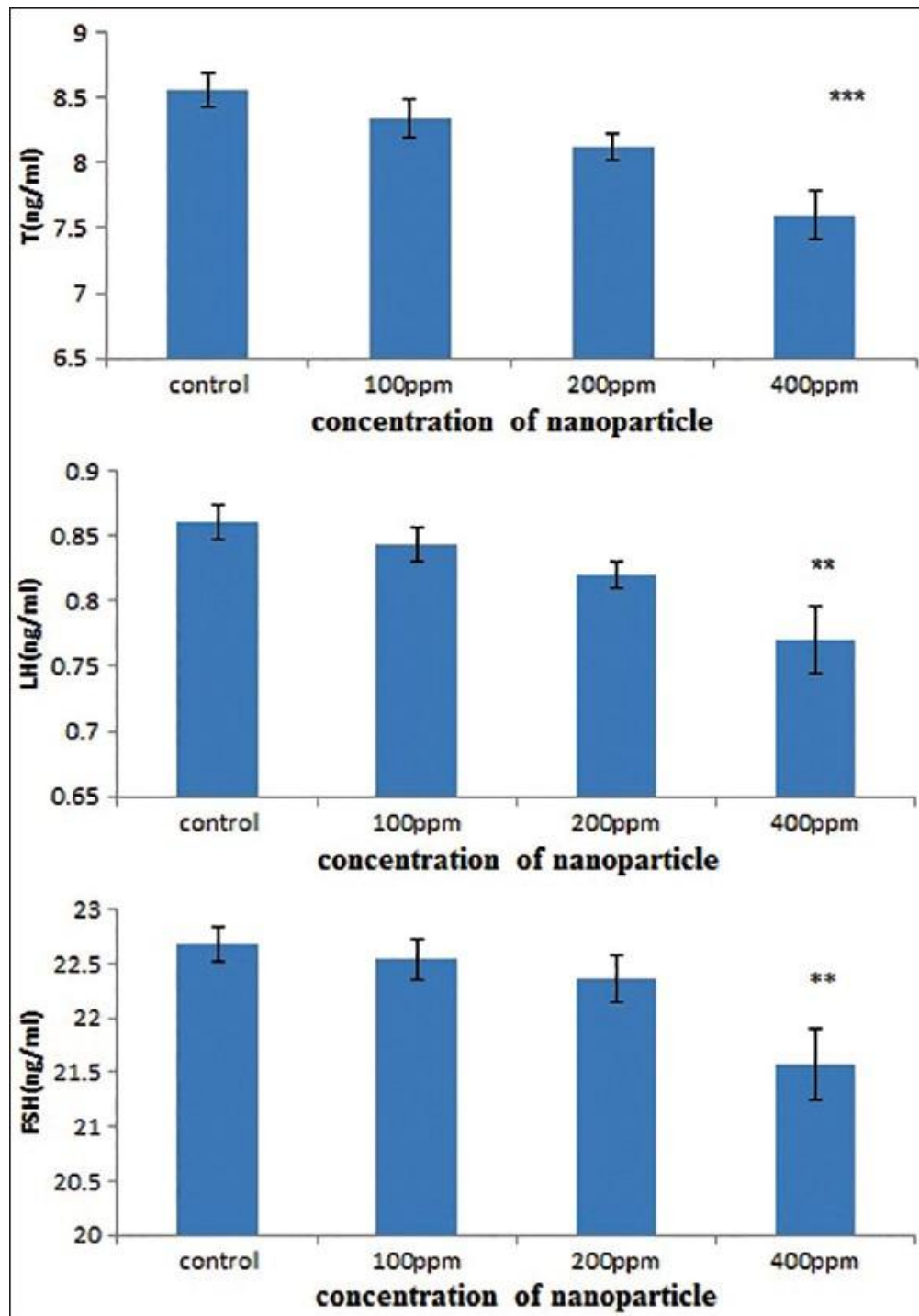
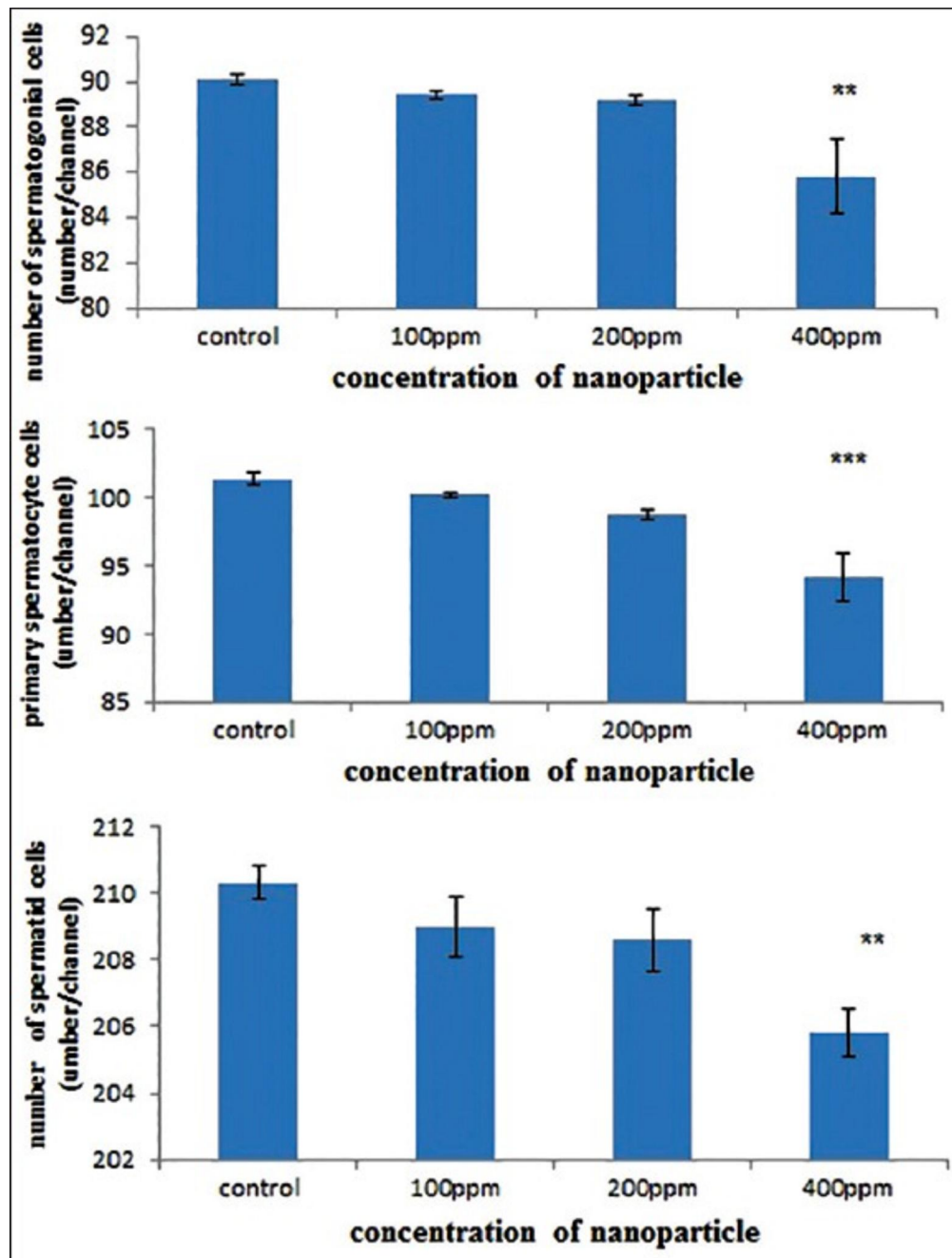
Figure 3Transmission electron microscopy image of Mn₂O₃ nanoparticles

Figure 4

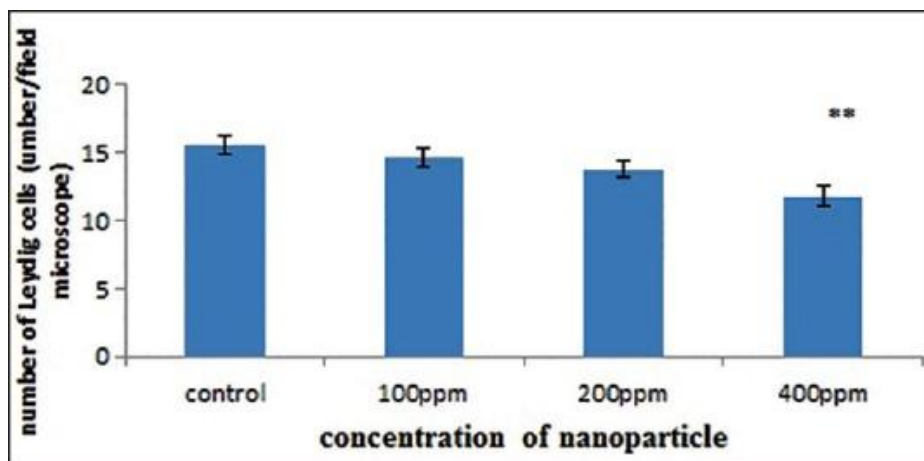


Mn₂O₃ nanoparticles effect on sex hormones

Figure 5

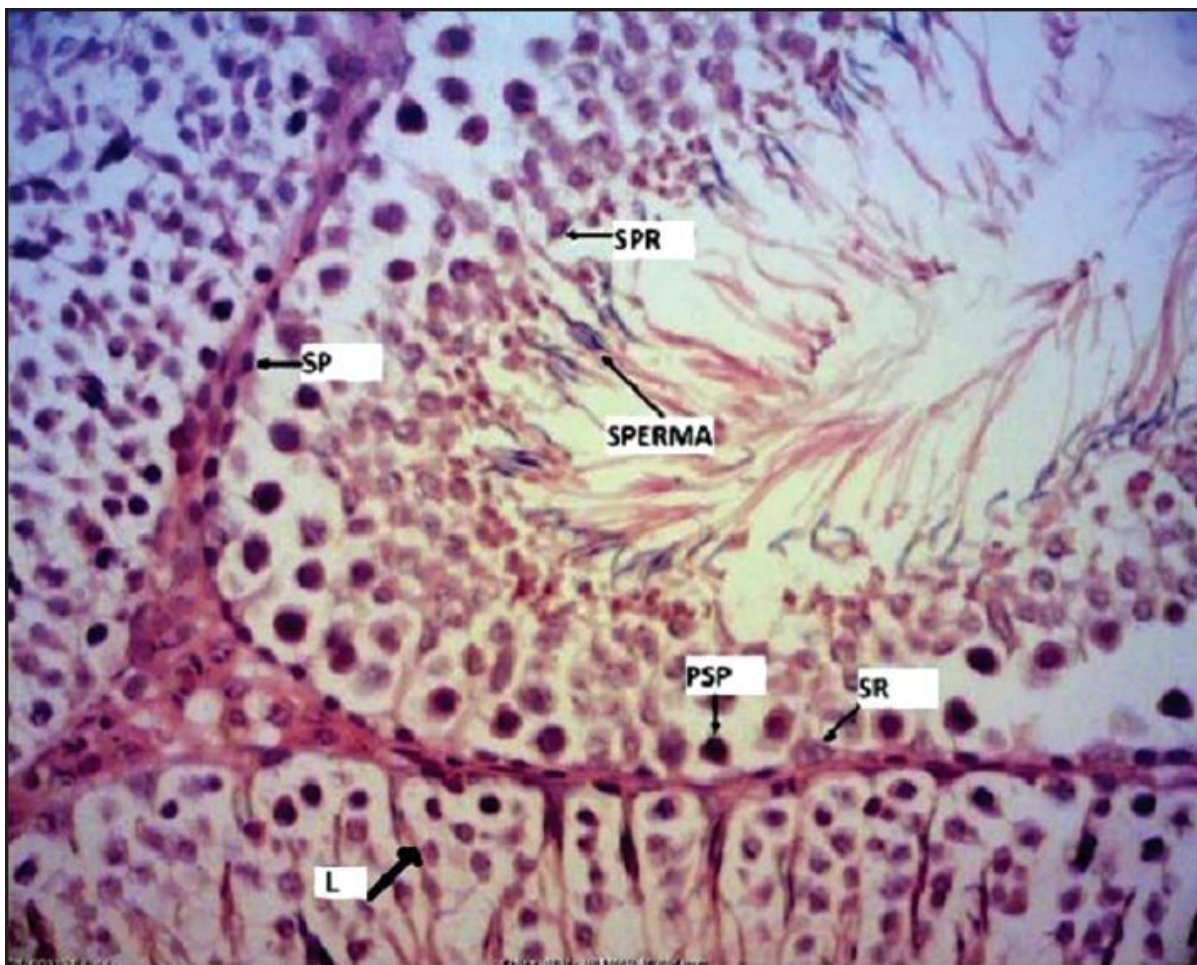


Mn₂O₃ nanoparticles, effect on testicle cell number

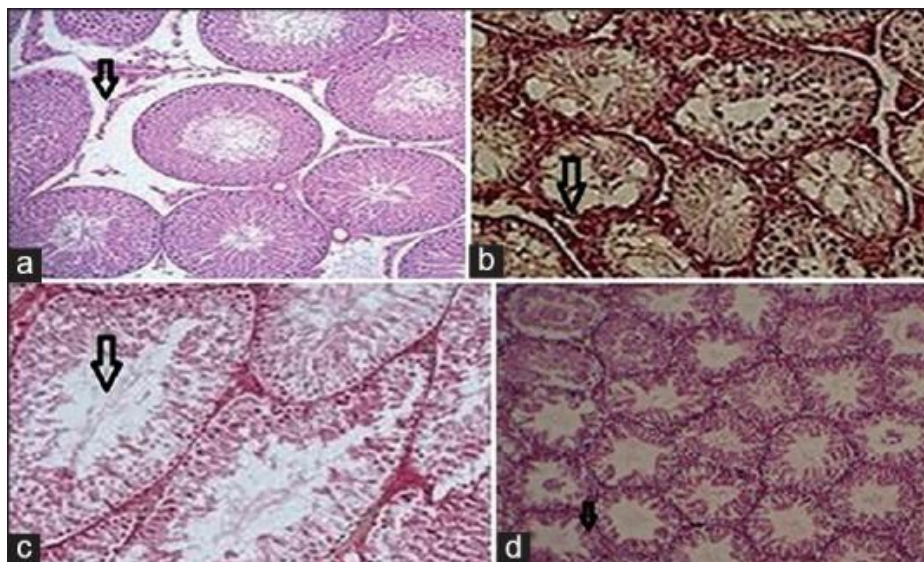
Figure 6

The number of cells in seminiferous tubules. The structure of rat testis tissue controls (H and E, $\times 40$). SP: spermatogonial cells, PSP: primary spermatocyte cells, SPR: Spermatid cells, L: Leydig cells, SPERMA: spermatozoide, SR: Sertoli cell

Figure 7



Mn₂O₃ nanoparticles, effect on number of Leydig cells

Figure 8

Effects of Mn₂O₃ nanoparticles over the damage of testis. (a) Arrows show elevation in cellular disruption of seminiferous tubules, interstitial edema, and decline in cell regulation were observed by H and E ($\times 10$). (b) Arrows show chaos in the germinal cells level in seminiferous tubules, increased in the gap between seminiferous tubular, and vacuoles seen in epithelium by H and E ($\times 10$). (c) Arrows indicate elevation in diameter of seminiferous tubules and decline in epithelium diameter were observed, H and E ($\times 10$). (d) Arrows indicate images of seminiferous tubules in the control-group demonstrated uniformity of the seminiferous tubules were seen, H and E ($\times 10$)

Articles from Journal of Natural Science, Biology, and Medicine are provided here courtesy of **Medknow Publications**